Interseismic Lithospheric Response of the Southern End of the Cascadia Subduction Zone Since the 1992 Cape Mendocino M 7.1 Earthquake

Jessie Vermeer[1]* and Mark Hemphill-Haley[2]

[1]U.S. Geological Survey, Earthquake Science Center, P.O. Box 158, Moffett Field, CA 94053
[2]Cal Poly Humboldt, Department of Geology, 1 Harpst St., Arcata, CA 95521
*jvermeer@usgs.gov

Introduction and background

The 1992 Ms7.1 (Mw 7.0) Cape Mendocino earthquake had no on-shore surface rupture, but caused a tsunami and crustal deformation with a maximum of 1.4 m of measured uplift along the nearby coast (maximum modeled coseismic uplift of 1.95 m, **Figure 1**), and up to 0.3 m of measured subsidence inland (maximum modeled coseismic subsidence of 0.43 m, **Figure 1**) (Oppenheimer et al., 1993; Carver et al., 1994; Murray et al., 1996). Coseismic deformation was measured with a leveling survey along the main roads (**Figure 1**), and by measuring the extent of the coastal intertidal organism die-off as a proxy for relative sea level change (**Figure 2**). In 2014-2015 we used geodetic Global Positioning System (GPS) benchmark observations and coastal observations to measure elevation change since the 1992 surveys to identify if there has been significant interseismic deformation (Vermeer, 2016). The results indicate there has been no detectable elevation change within the coseismic deformation area, suggesting that the 1992 earthquake likely occurred on a low strain rate fault and not the active subduction zone interface.

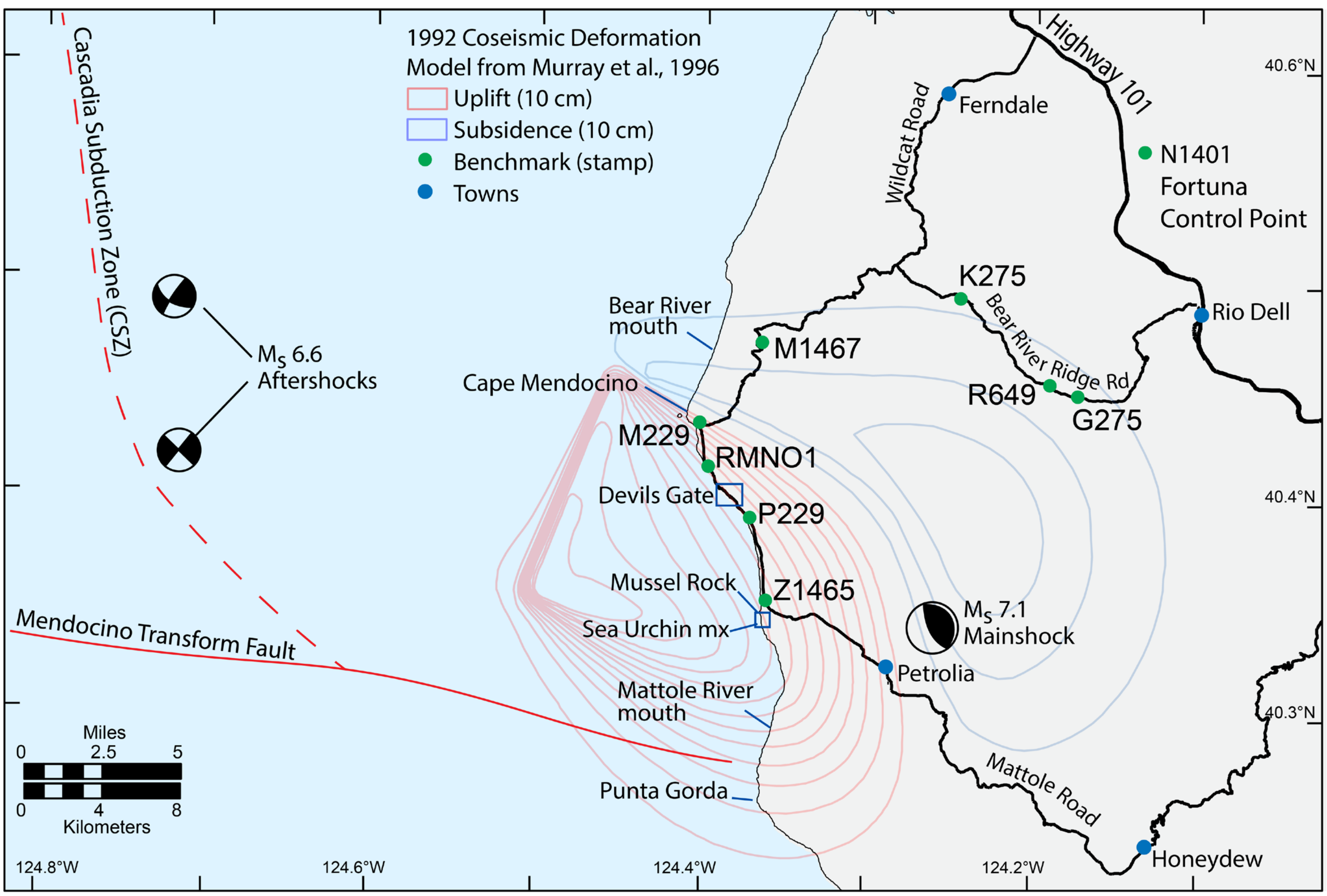

Figure 1. Map showing main roads, locations of significant landmarks along the coast, the benchmarks surveyed in this study, the locations of epicenters and focal mechanisms in the 1992 earthquake sequence (Oppenheimer et al., 1993), the Cascadia Subduction Zone and the Mendocino Transform Fault offshore, and the coseismic surface deformation contours (Murray et al., 1996).

Methods

GPS Measurements And Comparison To Leveling

In January to May 2015 we surveyed suitable benchmarks within the 1992 leveling survey using GPS for ~6 hours each with a Trimble Zephyr Geodetic antenna and Net R9 receiver (provided by UNAVCO) (Vermeer, 2016). The data were post-processed through OPUS to correct the position relative to nearby continuously operating GPS stations, yielding an elipsoid height relative to NAD83(2011) (NOAA, 2022) (**Figure 3A**). Orthometric elevations are defined by the height above the geoid. Ellipsoid height was converted to orthometric elevation using a geoid model (**Figure 3A**). Re-analysis of benchmark elevation change, using the measurements of Vermeer (2016) was done again in 2022 for this publication.

For this study we used two geoid models with different datums: GEOID18 produces a NAVD88 orthometric height, and xGEOID20B produces an orthometric height relative to the America-Pacific Geopotential Datum of 2022 (NA-DGD2022) (Ahlgren et al., 2020). GEOID18 is created by calibrating the gravimetric geoid to NAVD88 using GPS positions on benchmarks that also have leveling derived orthometric heights (Ahlgren et al., 2020). However, GEOID18 may not be the most appropriate geoid model for converting our 2015 benchmark GPS elipsoid heights to an orthometric elevation, because within the study area, 1992 post-seismic leveling was used to calibrate the geoid model against GPS benchmark observations collected in 2012. If any true benchmark elevation change had occurred between 1992 and 2012, the calibration process could potentially mask that elevation change. The other geoid option is xGEOID20B, a gravimetric geoid that is based on a variety of gravimetric measurements and is not tied to leveling-derived orthometric benchmark elevations (Ahlgren et al., 2020). Because it is not tied to the NAVD88 vertical datum, derived orthometric heights cannot be directly compared to the 1992 leveling elevations, so we used the Fortuna control point (benchmark N1401) as a study-specific datum to determine the height for each benchmark relative to the control point in 1992 and 2015, then difference the 1992 and 2015 relative elevations (**Figure 3B**). We chose this benchmark because it was included in the 1992 leveling survey, is located well outside the 1992 coseismic

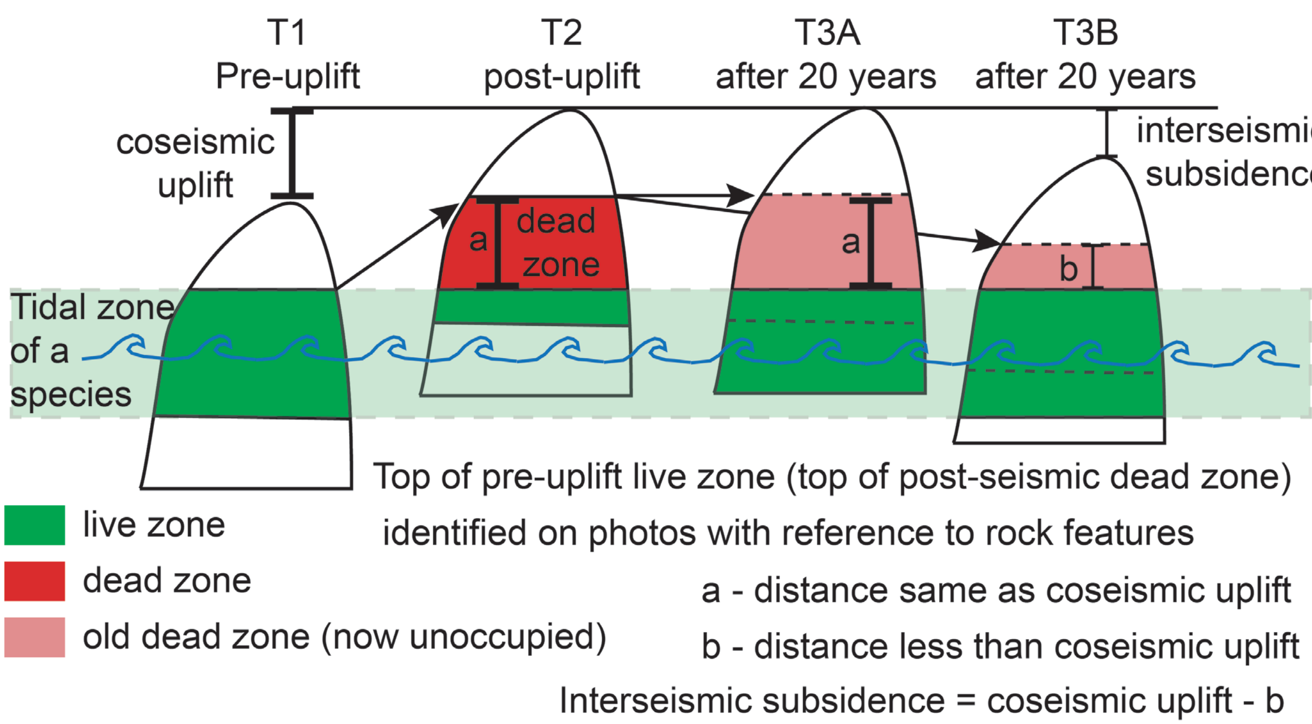

Figure 2. Schematic of intertidal organism live and dead zones through seismic cycle. T1) Before coseismic uplift, organisms are living with the whole colony within the appropriate tide level. T2) Coseismic uplift raises upper part of the colony out of the appropriate tide level, causing desiccation and death. If no early post-seismic rebound, dead zone height should be equal to coseismic uplift. T3A) If no interseismic subsidence, height from top of post-uplift dead zone to top of current live zone should be roughly equal to coseismic uplift. T3B) If there has been interseismic subsidence, height from top of post-uplift dead zone to top of current live zone should be less than coseismic uplift. The difference between b and the coseismic uplift equals the interseismic subsidence. T1 and T2 are modified from Carver et al. (1994), entire figure modified from Vermeer (2016).

deformation zone (no elevation change detected in 1992 compared to the previous survey) and was suitable for GPS position measurement.

Relative Sea Level Change Methods

Relative sea level change was measured using three methods: intertidal organism growth positions compared to post-earthquake photos, and growth positions of sea urchins relative to unoccupied urchin pits in the rocks, and 1992 to 2014-15 intertidal photo comparison at similar tide levels (Vermeer, 2016).

After the 1992 coseismic uplift, intertidal organisms that were lifted out of their ideal tidal zone died off, and measurements of the death zone height served as a proxy for relative sea level change resulting from crustal uplift (**Figure 2** T2) (Carver et al., 1994). Re-observation of specific sites that had been measured and photographed in 1992 allowed for comparison of intertidal organism growth positions between 1992 and 2014-15, a proxy for relative sea level change over that interval (**Figure 2** T3A and T3B) (Vermeer, 2016).

Sea urchins are mobile organisms that form pits on the rocks they occupy by physically eroding the rock using their teeth (R Rasmussen, Humboldt State University emeritus professor, personal communication, 2015). After the 1992 uplift, they abandoned the higher parts of rocks, leaving distinct fresh pits that were easily distinguished from older pits during observations in 2014-15 (**Figure 4B**) (Vermeer, 2016). Measurement of 2014-15 urchin locations relative to the fresh but unoccupied pits above them serves as a relative sea level change proxy (R Rasmussen, Humboldt State University emeritus professor, personal

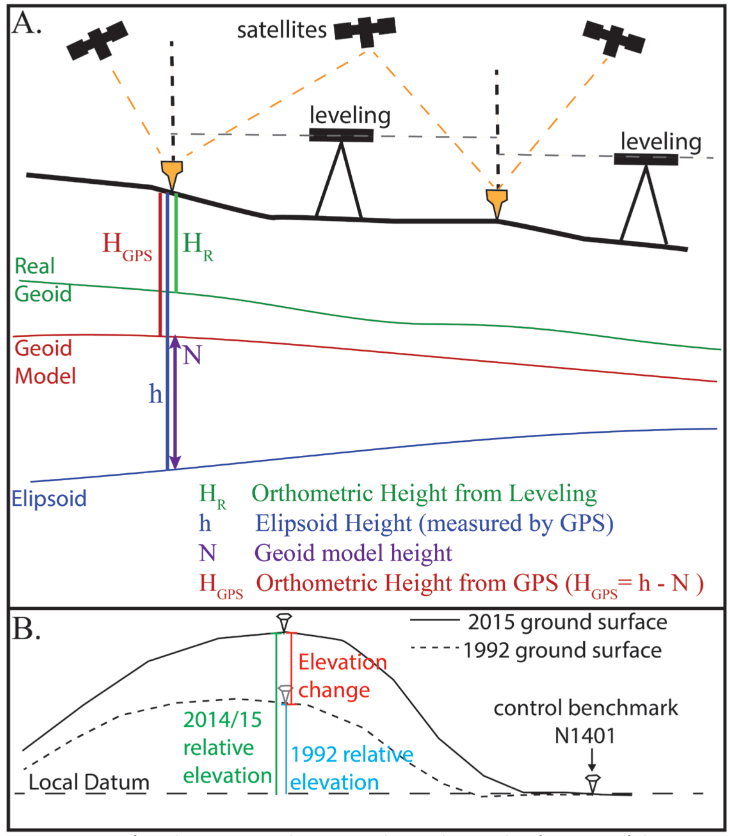

Figure 3. A) Schematic showing benchmarks (orange) being measured by GPS and leveling, and the various datums (real geoid, modeled geoid, and elipsoid). Leveling derived orthometric height is relative to the real geoid, while GPS derived orthometric height is relative to a modeled geoid. Most of the GPS measurement uncertainty comes from the difference between the real and modelled geoid height. B) Schematic of local datum based on control point outside the deformation area, and temporal elevation change.

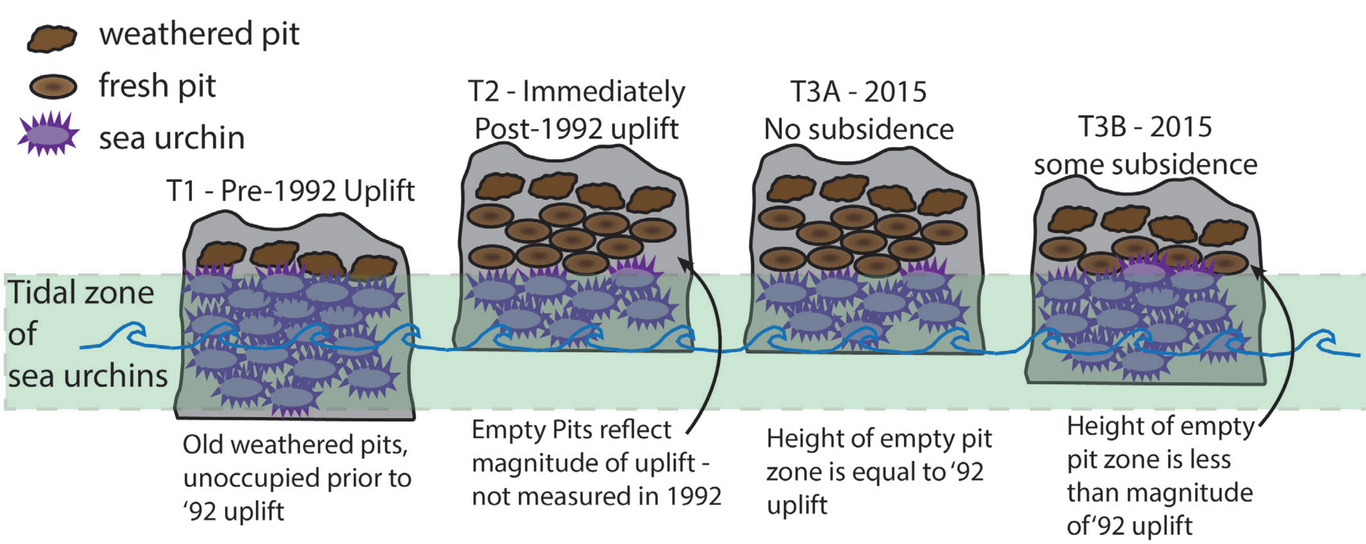

Figure 4. Sea Urchin fresh pits and living locations T1) before coseismic uplift, T2) after uplift, and 20 years later with T3A) no subsidence or T3B) some subsidence. Modified from Vermeer (2016).

communication, 2015). In this case, the height difference between the top of pre-1992 pits and current urchin position has to be compared to other measurements of coseismic uplift, and the difference indicates 1992-2014 relative sea level change (**Figure 4C** and **D**).

Some field photos provided from 1992 (A. Jayko, USGS, Personal Communication, 2015) have matching notes specifying the day and approximate time, and they capture distinctive rocks, calm water, and features that allowed for determination of the time the photo was taken (Vermeer, 2016). We then used tide charts and calculation of tide height between high and low tide peaks to determine the tide level at the time and location of the photo (New Zealand Nautical Almanac, 2013). In two instances, tide levels captured in the 1992 photos were appropriate to complete direct comparison of the tide height on the rocks between 1992 and 2014-15, limited by the accessible tide levels in 2014-15.

Results

Benchmark elevation change results

A total of 9 benchmarks were observed with GPS in 2015, including the control point in Fortuna (**Table 1**) (Vermeer, 2016). The elevation change of the benchmarks (**Figure 5** and **Table 1**) are within 1σ of zero change for all but one benchmark (M1467). No significant elevation change is detected using orthometric heights relative to the control point from either geoid model, or direct orthometric height comparison using the 1992 and GEOID18 NAVD88 orthometric elevations. The 0.038 m subsidence of M1467 may be due to slope instability. This benchmark was within the coseismic subsidence zone (**Figure 1**), so the expected interseismic tectonic signal would be up.

Relative Sea Level Change Results

In 2014-15, localized measurements of intertidal organisms were made at 5 locations at Mussel Rock where photos from 1992 could be matched (**Figure 1**). The relative sea level change suggested by the measurements is highly variable among these sites. The maximum suggests 0.6 m of subsidence, while one site suggests 0.3 m of uplift since 1992; the average is 0.23 m of subsidence.

The 2014-15 position of sea urchins (12 measurements) averaged 142 cm lower than their pre-1992 pits. This average is approximately equal to the coseismic uplift measured at Mussel Rock (1.4 m, Carver et al., 1994) immediately to the north, indicating there has been no detectable relative sea level change since 1992. The precision of this relative sea level proxy is probably ~0.2 m but may be affected by complicated local wave splash dynamics (R Rasmussen, Humboldt State University emeritus professor, personal communication, 2015).

The tide photo comparison was completed at two locations and indicate the 2014-15 relative sea level is within ~0.1 m of the post-uplift 1992 relative sea level (Vermeer, 2016). More photo comparisons could not be completed because 2014-15 tides were not sufficiently low to match the photographed 1992 tides, because there were exceptionally low tides in the region during the 1992 survey.

Table 1. Benchmark orthometric heights and elevation change, 2015 – 1992. Benchmark position data from NGS

		Orthometric height			Benchmark height relative to control benchmark (bm elev - control bm elev)			2015 - 1992 elevation difference					
PID	Stamp	2015 xGEOID20B ortho ht	2015 GEOID18 NAVD88 ortho	1992 leveling ortho elev (NAVD88)	2015 xGEOID20B relative to control	2015 GEOID18 relative to control	1992 relative to control	xG20b - 1992 Relative to control elevation difference (m)	G18-1992 Relative to control elevation difference (m)	G18 - 1992 ortho elevation difference (m)	OPUS solution ellipsoid ht accuracy (NAD83)	xGEOID20B ortho ht accuracy from geoid calculator	GEOID18 ortho ht accuracy from OPUS
LV0661	N 1401	75.367	76.314	76.301				-0.934	0.013	0.013	0.012	0.023	0.050
LV1251	Z1465	8.352	9.275	9.261	-67.015	-67.039	-67.040	0.025	0.001	0.014	0.023	0.019	0.070
LV0368	P 229	8.255	9.174	9.169	-67.112	-67.140	-67.132	0.020	-0.008	0.005	0.008	0.019	0.052
LV1255	JAG RMN01	9.746	10.677	10.676	-65.621	-65.637	-65.625	0.004	-0.012	0.001	0.000	0.018	0.049
LV0366	M 229	92.932	93.872	93.880	17.565	17.558	17.579	-0.014	-0.021	-0.008	0.003	0.018	0.050
LV1263	M 1467	156.408	157.370	157.380	81.041	81.056	81.079	-0.038	-0.023	-0.010	0.005	0.018	0.049
LV0405	R 649	680.687	681.609	681.615	605.320	605.295	605.314	0.006	-0.019	-0.006	0.001	0.021	0.047
LV0404	G 275	689.865	690.785	690.790	614.498	614.471	614.489	0.009	-0.018	-0.005	0.004	0.021	0.048
LV0410	K 275	613.099	614.035	614.051	537.732	537.721	537.750	-0.018	-0.029	-0.016	0.008	0.019	0.047

Discussion

Benchmark Survey

The measured benchmark orthometric and relative elevation changes indicate there has been no measurable vertical crustal deformation since the 1992 post-seismic survey. Because the xGEOID20B orthometric heights cannot be directly compared to the 1992 leveling orthometric heights, without a control point outside the CSZ deformation zone we cannot determine if there is an elevation change signal over a larger geographic area.

Relative Sea Level Measurements

Mussel rock was the only area with photos from the 1992 survey appropriate for making 2014-15 comparisons. Unfortunately, the intertidal organism population at Mussel Rock in 2014-15 was relatively sparse and unhealthy. This may be due to regional environmental factors (short-term or long-term sea temperature change or localized summer sand persistence through winter), intertidal water flow and splash dynamics, or local delay of post-uplift recolonization (R Rasmussen, Humboldt State University emeritus professor, personal communication, 2015).

The sea urchin position measurements indicated little to no land subsidence since 1992, in agreement with the benchmark survey. Likewise, the photo tide comparisons indicated no detectable relative sea level change since post-seismic 1992. These measurements were made south (near Mattole River mouth) and north (Devils Gate) of Mussel Rock in areas of lower coseismic uplift where lower interseismic subsidence would be expected.

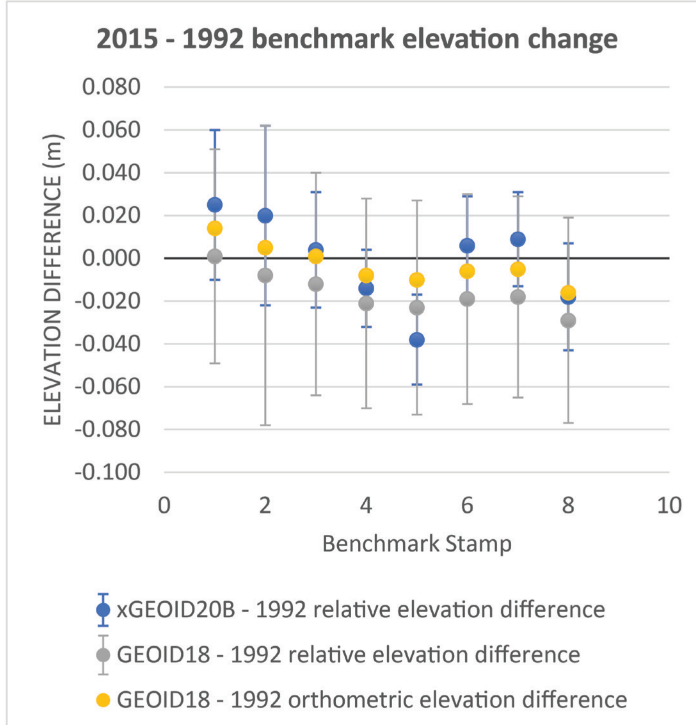

Figure 5. benchmark elevation change calculated relative to the control point (N1401), or by directly differencing orthometric heights from GEOID18. Error bars are 1σ and include GPS elipsoid height accuracy plus geoid orthometric height accuracy. The accuracy of the control point, N1401, is not propagated through the relative elevation change calculations, but would effectively increase the size of the 1σ error bars. Only M1467 has elevation change greater than the 1σ accuracy, all other benchmarks have elevation change that is less than the measurement accuracy.

The intertidal organism relative sea level proxies could be implemented with more precision if the 1992 total station vertical extent of mortality survey data could have been incorporated. With the current methods, the measurements are sparse making them particularly susceptible to variability from site effects like wave splash dynamics and sand levels. Additionally, the sparseness of intertidal organisms in 2014-15 brings into question how robust these measurements are. Currently, the results are interpreted to indicate little (<0.3 m) to no relative sea level change since 1992, but additional work is necessary to make any high-confidence interpretations.

Tectonic Significance

Relative to the 1992 earthquake, the elevation change measurements presented here are early in the seismic cycle, when we would expect the greatest post-seismic or inter-seismic recovery of coseismic crustal deformation, especially if this earthquake was related to a rapid-loading Cascadia Subduction zone (CSZ). Because of the imprecision of the model geoid orthometric elevation conversion, the vertical deformation would have to be greater than ~1 mm/yr to be detected using these methods over this time period. The lack of measurable vertical deformation may indicate the 1992 source fault is a low strain rate subsidiary crustal fault, consistent with seismic imaging of the subduction zone geometry (McCrory et al., 2012). However, if the post-1992 local deformation and regional CSZ deformation were acting in opposite directions, they could potentially cancel each other out. Since the benchmark survey is measured against a local datum, it would be unable to capture deformation on a larger wavelength than the study area, so it may not have captured any CSZ-related deformation. However, the Cape Mendocino and nearby continuous GPS stations also indicate little to no vertical deformation is occurring relative to the North American plate, suggesting that even the contemporary CSZ-related vertical deformation is occurring very slowly.

References

Ahlgren K., G. Scott, D. Zilkoski, B. Shaw, N. Paudel, NOAA Technical Report NOS NGS 72 GEOID 18, 2020, https://geodesy.noaa.gov/library/pdfs/NOAA_TR_NOS_NGS_0072.pdf.

Carver, G.A., Jayko, A., Valentine, D.W., and Li, W.H., 1994, Coastal uplift associated with the 1992 Cape Mendocino earthquake, northern California: Geology, v. 22, p. 195–198, doi: 10.1130/0091-7613(1994)022<0195:CUAWTC>2.3.CO;2.

GEOID18, NOAA National Geodetic Survey, https://www.ngs.noaa.gov/GEOID/GEOID18/ last accessed July 12, 2022.

McCrory, P. a., Blair, J.L., Waldhauser, F., and Oppenheimer, D.H., 2012, Juan de Fuca slab geometry and its relation to Wadati-Benioff zone seismicity: Journal of Geophysical Research: Solid Earth, v. 117, p. 1–23, doi: 10.1029/2012JB009407.

Murray, M.H., Marshall, G.A., Lisowski, M., and Stein, R.S., 1996, The 1992 M = 7 Cape Mendocino, California, earthquake: Coseismic deformation at the south end of the Cascadia megathrust: Journal of Geophysical Research, v. 101, p. 17707, doi: 10.1029/95JB02623.

New Zealand Nautical Almanac, 2013, Method to find times or heights between high and low waters, p. 32 – 34.

NOAA, 2022, Online Positioning User Service (OPUS), https://www.ngs.noaa.gov/OPUS/ last accessed: July 12, 2022.

Oppenheimer, D.H., Beroza, G., Carver, G.A., Dengler, L., Eaton, J., Gee, L., Gonzalez, F., Jayko, A., Li, W.H., Lisowski, M., Magee, M., Marshall, G.A., Murray, M.H., McPherson, R.C., et al., 1993, The Cape Mendocino, California, Earthquakes of April 1992: Subduction at the Triple Junction: Science, v. 261.

Vermeer, J.L., 2016, Interseismic lithospheric response of the southern end of the Cascadia Subduction Zone since the 1992 Cape Mendocino m 7.1 earthquake, Master of Science Thesis, Humboldt State University.

xGEOID20, Experimental Geoid Models 2020, NOAA National Geodetic Survey, https://beta.ngs.noaa.gov/GEOID/xGEOID20/index.shtml last accessed July 12, 2022.

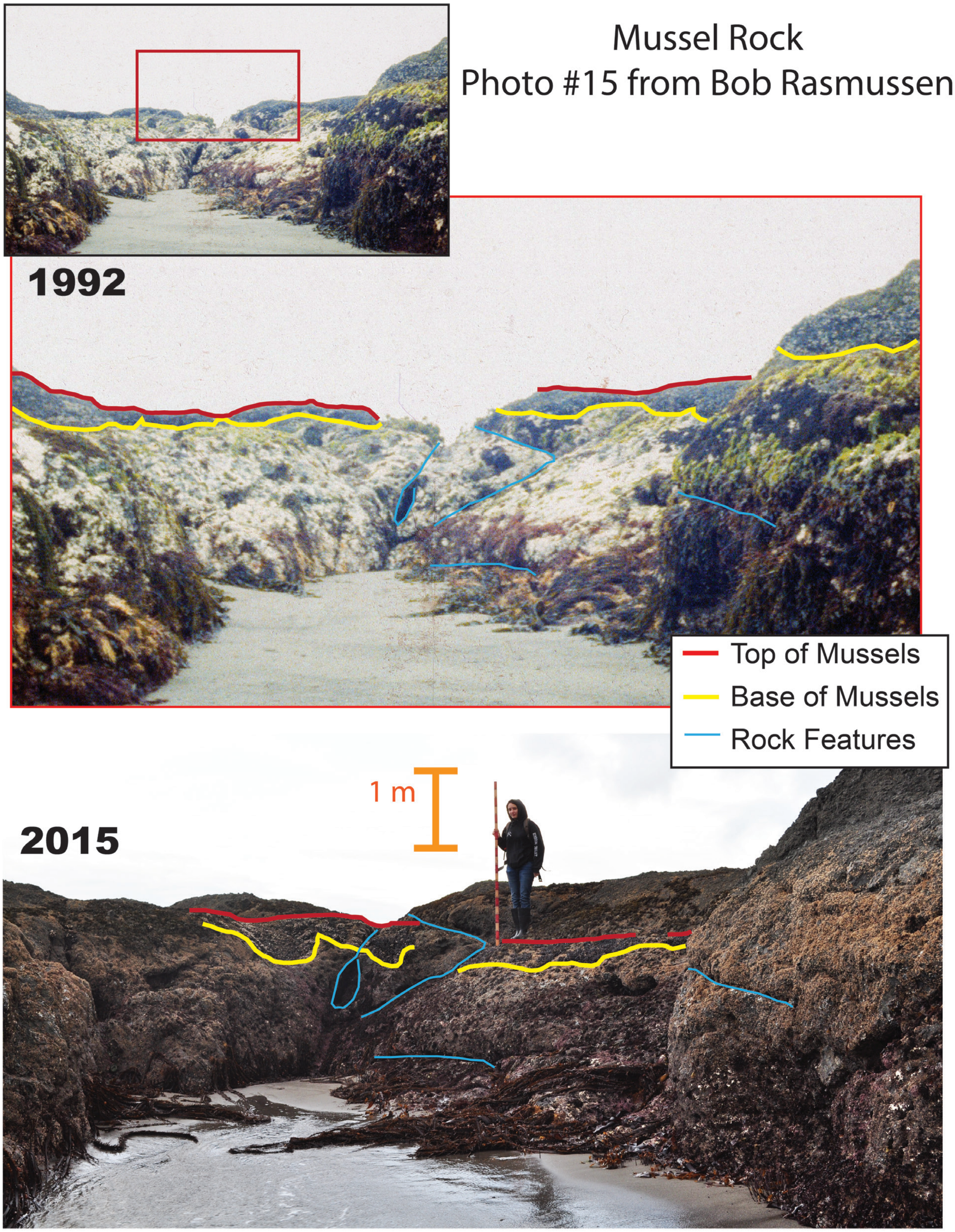

Figure 6. Example of methods and results for comparison of intertidal organism position. 1992 photo with top (red) and base (yellow) of pre-uplift mussel colony location, and distinctive rock features (blue) marked. 2014-15 photo of the same location with mussel colony identified (same annotation colors). Position of the colony is compared to the 1992 position using rock features as a reference frame. 1992 photo from R. Rasmussen, 2015 photo from Vermeer (2016)